CORRELATING NIR SPECTRA AND LROC NAC PHOTOMETRIC DATA AT SITES OF DIRECT PLAGIOCLASE DETECTION. Anna R. Schonwald[1], Timothy M. Hahn Jr.[1], Ryan M. Watkins[2], Bradley L. Jolliff[1], [1]Washington University in St. Louis, Department of Earth and Planetary Sciences, Campus Box 1169, 1 Brookings Drive, Saint Louis, MO 63130, United States, [2]Planetary Science Institute, Tucson, AZ 85719, United States.

Introduction: The formation of an ancient, plagioclase-rich flotation crust is predicted by the lunar magma ocean hypothesis, where density disparities drive crystal-melt segregation of plagioclase and cogenetic mafic melt. Plagioclase-rich rocks have been detected in the central peaks and uplifted rims of large craters and impact basins within the lunar highlands [1-4]. We use "pure anorthosite" (98 to 95 wt.% plagioclase) and "purest anorthosite" (>98 wt.% plagioclase) to classify variations in areas where plagioclase-rich rocks have been detected by a distinct spectral absorption at 1250 nm [1], which can be masked by small amounts of mafic minerals (~7% by volume in the laboratory) [5].

Spatially correlated near infrared (NIR) spectra and single scattering albedo (SSA) can be used to characterize variations in SSA as a function of mafic mineral content and help determine the spatial extent and purity of anorthosites. Here, we investigate five sites on the lunar far side with confirmed exposures of pure anorthosite [1-4, Fig. 1] using multiple Lunar Reconnaissance Orbiter Camera (LROC) Narrow Angle Camera (NAC) derived datasets (e.g. NAC digital terrain model (DTM), slope maps, and SSA maps) and Moon Mineralogy Mapper (M^3) hyperspectral images.

Data and Methods: We use the USGS's Integrated Software for Imagers and Spectrometers (ISIS3) to prepare the images for Hapke Modeling. The LROC NAC reflectance data is resampled to the NAC DTM resolution (~5 m/px). We use the resampled LROC NAC reflectance data, NAC DTMs and the illumination geometry of each image to calculate the incidence and emission angle for each pixel [6,7]. The local illumination geometry is then used in the Hapke modeling to calculate the single-scattering albedo (SSA).

The Hapke equation models the reflectance on the lunar surface and other solar system bodies [8]. We make simplifying assumptions about parameters (e.g., grain size, space-weathering maturity) so this model can be used across the lunar near and far side [8,9]. We calculate SSA (*w*) using a two-parameter optimization algorithm [10].

We apply the ground-truth correction to L2 Moon Mineralogy Mapper (M^3) data [11] and use the continuum removal tool in ENVI version 5.5 (Exelis Visual Information Solutions, Boulder, Colorado) to better identify weak spectral absorptions.

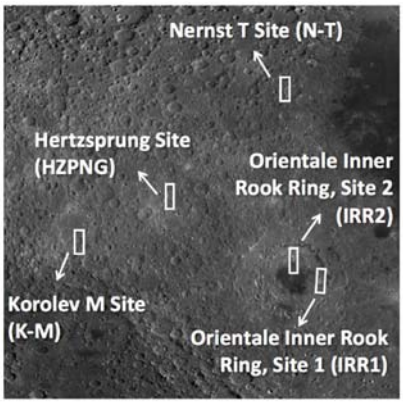

Figure 1: Geologic context of the five sites, WAC basemap, equirectangular projection.

Sites (left to right): Korolev-M (K-M), 8.49°S, 202.69°E; Hertzsprung (HZPNG), 5.62°N, 229.7°E; Nernst-T (N-T), 36.17°N, 263.05°E; Orientale Inner Rook Ring site 2 (IRR2), 11.26°S, 264.11°E, and site 1 (IRR1), 19.47°S, 273.38°E.

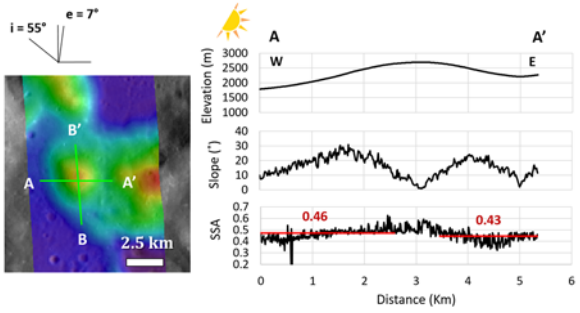

Figure 2: Transect across a uniform massif in HZPNG. The average SSA on the sun-facing slope is only 0.03 higher than the non-sun-facing slope, indicating that topography is not a significant contribution to variation in derived SSA.

Results: The correction for local slopes and illumination geometry using NAC DTMs greatly reduces the effect of solar illumination on the derived SSA values (Fig. 2). At each site where pure plagioclase absorptions were identified the topography-corrected SSA values range from 0.54 to 0.64 and correspond to Clementine FeO contents generally <2.9 wt.% and (based on preliminary mass balance) >88 vol.% plagioclase (Fig. 3).

Variations in regolith maturity affect the computed SSA values; e.g., fresh craters or outcrops on steep slopes have SSA values as high as 0.86. We interpret SSA variations in areas that do not appear to be affected by maturity (i.e., mature surfaces and low slopes) to result from variations in the quantity of mafic rock components mixed with plagioclase. We further investigate these variations by correlating SSA to

variations in mafic content determined from M^3 spectra.

Variations in SSA and M^3 spectra show mixing trends on slopes from more mafic to plagioclase-rich material (Fig 4). Areas with strong plagioclase absorptions features or featureless spectra exhibit SSA values >0.54. Mg-Al spinel was identified at three of the five sites studied, in some areas plagioclase/spinel mixtures exhibit similar SSA to plagioclase-rich areas.

Discussion: From the data, we infer that areas with plagioclase absorption features that correlate with SSA values of 0.6 and above are likely areas of pure plagioclase. Areas where spectral absorption features and SSA values do not correlate likely reflect variations in maturity or other physical parameters. Using M^3 spectra and SSA as layered datasets we can evaluate compositional and mineralogical variations on an outcrop scale. Each of the sites investigated exhibit high variation in local materials suggesting that more mafic rocks occur with areas of pure anorthosite. The most concentrated and extensive areas of pure anorthosite are found in IRR1.

Acknowledgements: We thank NASA for support of the LRO extended mission and for the great work of the LRO and LROC Operations Teams.

References: [1] Ohtake, M. et al. (2009) *Nature, 461* (7261), 236-U110. [2] Cheek, L. et al. (2013) *JGR*, *118*(9), 1805-1820. [3] Hanna, K. L. D., et al. (2014) *JGR*, *119*(7), 1516-1545. [4] Yamamoto, S., et al. (2015) *JGR*, *120*(12), 2190-2205. [5] Cheek, L. and C. Pieters (2014) *Am. Mineral.*, *99*(10), 1871-1892. [6] Clegg-Watkins R.N. et al. (2016) *Icarus, 273*, 84-95. [7] Clegg-Watkins, R.N., et al. (2017) *Icarus*, *285*, 169-184. [8] Hapke, B.W. (2012a) *Icarus*, *221*(2), 1079-1083. [9] Hapke B. W. (2012b), Theory of Reflectance and Emittance Spectroscopy (2nd Ed.). [10] Hahn Jr., T.M. et al. (2014), 48th LPSC,. #2837. [11] Pieters, C. M., et al. (2009) *Current Science*, *96(4),* 500-505. [12] Spudis, P. D. et al. (2014) *JGR, 119*(1), 19-29.

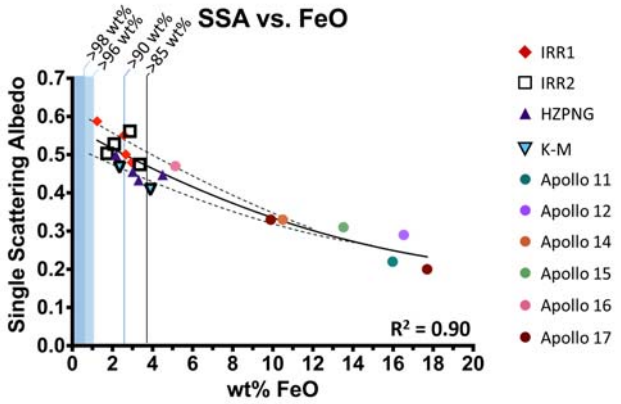

Figure 3: Correlation between SSA and wt% FeO. Apollo sites use average FeO values from sample compositions [10], plagioclase sites use Clementine FeO. Simple mass balance models for ferroan anorthosite estimate plagioclase content for wt% FeO.

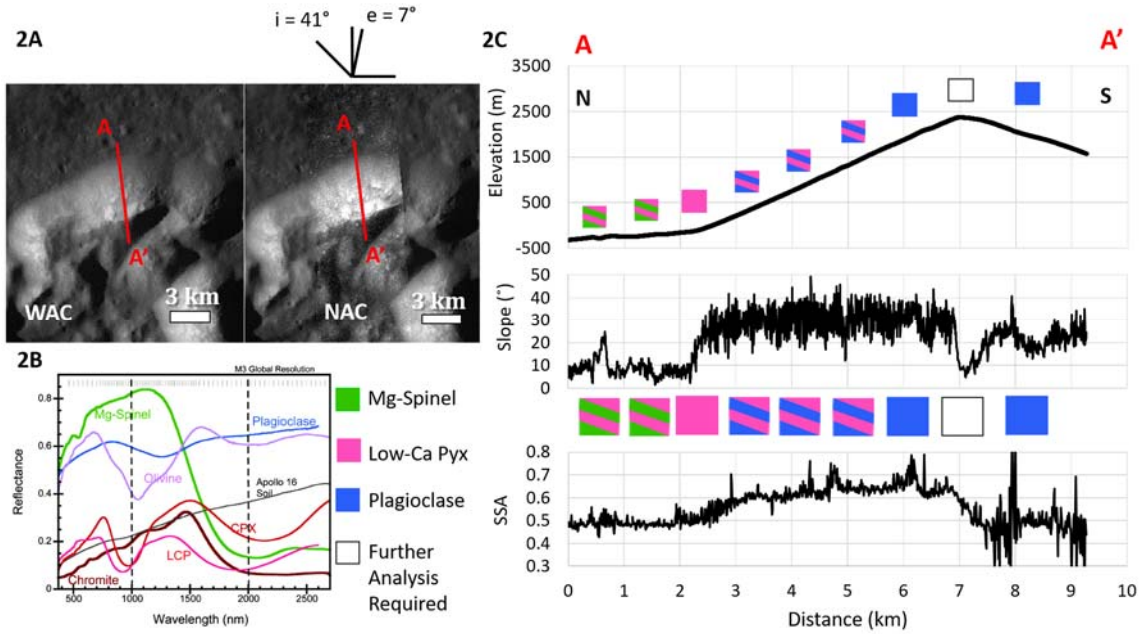

Figure 4: A) Geologic Context for the profile B) Diagnostic spectra from [5] with legend C) spatially correlated profile from the Maunder Formation [13] across a plagioclase-rich massif in IRR1.